

## RESEARCH ARTICLE

# The impact of glass powder on surface and morphological properties of Alumix 431 alloy

Ayşe Nur Acar<sup>\*1</sup>, Dogan Kaya<sup>2,3</sup>, Abdul Kadir Ekşi<sup>4</sup> and Ahmet Ekicibil<sup>2</sup><sup>1</sup>Çukurova University, Ceyhan Engineering Faculty, Mechanical Engineering Department, Adana, Türkiye<sup>2</sup>Çukurova University, Art and Science Faculty, Physics Department, Adana, Türkiye<sup>3</sup>Çukurova University, Graduate School of Sciences, Department of Advances Materials and Nanotechnology, Adana, Türkiye<sup>4</sup>Çukurova University, Engineering Faculty, Mechanical Engineering Department, Adana, Türkiye

## Article Info

### Article history:

Received: 31.12.2023

Revised: 30.04.2024

Accepted: 10.06.2024

Published Online: 27.06.2024

### Keywords:

Al-7xxx alloys,  
Alumix 431 alloy  
Waste glass powder  
Powder metallurgy  
Structural property,  
Surface morphology

## Abstract

The Al-7xxx series alloys exhibit exceptionally high strength, superior corrosion resistance, and excellent finishing characteristics. These qualities make them a common choice for manufacturing automotive and aerospace components. To further improve the mechanical and structural properties of these alloys, they are often reinforced with alloy powders. This study focuses on Alumix 431, an alloy of Al-7xxx series, combined with glass powder obtained from the grinding of waste glass. The primary aim of this research is to evaluate the use of glass powder as a reinforcement material in metallic alloys, such as aluminium alloys, with a particular emphasis on utilizing waste materials. The effect of glass powder on the surface and structural properties of Alumix 431 were investigated. A homogeneous mixture was obtained by blending the alloy with 15% (wt) glass powder. This mixture was then subjected to a shock pressure of 0.6 tons and underwent a heat-treatment process at 650 °C in a furnace for a 1 hour. The physical properties of the composite material-including hardness, density, surface topography, and microstructure- were characterized using optical microscopy, scanning electron microscopy, energy-dispersive X-ray spectroscopy, and X-ray diffraction analysis. The addition of glass powder to the alloy led to enhanced hardness and density. The maximum hardness and bulk density values were achieved with the Alumix 431-15% GP alloy, measuring 41.846 N/mm<sup>2</sup> and 2.451 g/cm<sup>3</sup>, respectively. Conversely, the lowest values for apparent porosity and water absorption found to be 2.293% and 0.935%, respectively. Furthermore, the study identified the formation of various phases, such as Al<sub>2</sub>CuMg, diopside, cristobalite, between Alumix 431 and the glass powder.

## 1. Introduction

Al-7xxx series alloys are widely used in industrial areas, including automotive and aerospace, due to their excellent mechanical and physical properties. These properties include high strength and toughness, excellent finishing characteristics and good corrosion resistance [1-3]. Primarily composed of zinc, these alloys can be strengthened through heat treatment and reinforced with other alloys or ceramic powders [2, 3]. The inclusion of magnesium and copper content in chemical composition enhances the thermal deformation properties, welding performance, corrosion resistance and specific strength of these alloys [3]. Aluminium alloys that contain ceramic additives are defined as aluminium matrix composites. The producing of these composite materials, powder metallurgy method has attracted attention for researchers due to some of advantages of this method such as obtaining net and/or near net shape, serial production, cheaply, avoiding interfacial reactions and decreasing undesirable reaction between the reinforcement and the matrix [4]. Alumix 431, an Al-7xxx series alloy, mainly consists of zinc, magnesium and copper, making it a high strengthened alloy [5]. Zinc is added to the aluminium for the promoting precipitation hardening due to its excellent solubility in the aluminium [5]. To enhance the wetting behaviour of aluminium's liquid phase and promote precipitation hardening with magnesium element, aluminium alloy is blended with copper element [5]. Finally, even a small addition of

magnesium, as little as 0.5 wt%, is incorporated into the aluminium alloy for affecting positively on the shrinkage by reducing oxide formation, enabling metal/metal contact and allowing diffusion [5, 6]. There are studies about alloy and composite material obtained from this alloy [1, 2, 5, 7-9]. Authors pressed Alumix 431 powders on the 400 MPa pressure and sintered at different temperatures (580-620 °C) and investigated the effect of pressure on the mechanical properties of this alloy. It was observed that when sintering temperature increased, sintering density of this alloy increased. The maximum sintered density obtained as 2.76 g/cm<sup>3</sup> at 610°C temperature [1]. Authors examined the density properties, mechanical strength and sintering characterization of this alloy prepared by traditional pressing and sintering techniques in various pressures and temperatures. Firstly, alloy samples prepared between 300 and 500MPa at 50 MPa intervals and 80°C temperature, secondly, samples produced under conditions of 230 MPa at RT and 180 MPa at 80°C temperature. Authors observed that dimensional change in warm compacted samples has lower than that of cold compacted samples. Mechanical strength of warm and compacted samples were recorded as almost equal [5]. Authors investigated the influence of B<sub>4</sub>C on the density properties of Alumix 431 alloy. It was revealed that sintering with participation of liquid phase was affected by addition of B<sub>4</sub>C. and sintering process of these samples also caused to densification of the material [9].

Waste glass powder is obtained by grinding of waste glass cracks and consisted of silica, soda ( $\text{Na}_2\text{O}$ ) and lime (such as  $\text{CaO}$ ) and other alkali oxides such as  $\text{MgO}$  [10-12]. Glass powder has pozzolanic features, which are reducing porosity and water absorption, owing to high amount of silica [13, 14]. As sodium oxide ( $\text{Na}_2\text{O}$ ) is added to silica, each positive sodium ( $\text{Na}^+$ ) ion becomes linked to a negative oxygen ( $\text{O}^{2-}$ ) of a tetrahedron, therefore decrease the cross-linking. This addition of  $\text{Na}_2\text{O}$  in to the silica has a role on the taking place some of the covalent bonds among the tetrahedra with ionic bonds [15]. Thus increases the flowability of the melt. But, calcium oxide ( $\text{CaO}$ ) is also added to balance and improve the insolubility of the melting [16]. Glass powder is applied as coating and adding agents into the structural and alloy materials because of its chemical composition [17, 18]. There are studies about glass powder and aluminium composite materials [19-21]. Authors prepared aluminium (Al-6061) matrix composite reinforced with glass powder changing from 0% to 30% using stir-casting method and characterized with mechanical, thermal and structural properties of these composite materials. They observed that when glass powder content increased in the Al-matrix, mechanical properties of composite samples improved and good bonding among matrix and reinforcement samples were also enabled [19]. Authors produced alumina-aluminium composite materials with glass powder by insitu method and aluminium based composite materials occurred using dissolution of alumina particles and Si and Cu alloying elements. Alumina particles acquired from mixture of copper and alumina oxides have bigger particles than that of copper oxides and glass powders in the mixtures including of more than 50% copper oxide particles did not stick together to form glassy structured globs [20]. Authors studied workability behaviour of Al-glass powder composite samples produced by powder metallurgy method. Al matrix mixed by 0-8% glass powder with particle size of  $60\mu\text{m}$ . When glass powder amount in the Al matrix increased, mechanical strength of composite samples increased owing to reduce of porosity and increase density [21]. With our study, it is aimed to evaluate of waste materials by using glass powder as an additive material into the metallic alloys prepared by traditional manufacturing method with high sintering temperature and examine the effect of glass powder (15% wt) on the physical, surface and microstructural morphology of Alumix 431 alloy. With our study, it is also purposed that physical and morphological properties will be reach to high values and improve at low temperature by preparing composite sample.

## 2. Materials and methods

The chemical composition of Alumix 431 powder acquired from Ecka Granules in Germany was given as 89% Al, 5.5% Zn, 2.5% Mg, 1.5% Cu and 1.5% lubricant [5, 7]. The chemical composition (wt%) of glass powder obtained from Acar Frit, Masse and Industrial Raw Materials Industry and Trade Limited Company in Kütahya, Türkiye were given as 68.26%,  $\text{SiO}_2$ , 1.58%  $\text{Al}_2\text{O}_3$ , 0.09%  $\text{Fe}_2\text{O}_3$ , 0.08%  $\text{TiO}_2$ , 8.54%  $\text{CaO}$ , 4.18%  $\text{MgO}$ , 15.52%  $\text{Na}_2\text{O}$ , 0.21%  $\text{K}_2\text{O}$  and 1.54% other substances recorded using HITACHI SEA 1200 VX model XRF device with 15kV of tube voltage and  $1000\mu\text{A}$  of tube current at vacuum medium. Alumix 431 powder was blended with 15% (wt) of glass powder to create a homogeneous of Alumix 431 and glass powder mixture. This mixture was pressed under 0.6 ton shock pressure, pressed and sintered at a temperature of  $650^\circ\text{C}$  in furnace for 1 hour. After sintering, the sample cooled to room temperature in the furnace. As control sample, Alumix

431 sample that did not mixed with glass powder was also prepared in this same procedure. The physical properties of both the composite material and the control sample were investigated. Hardness measurements were performed by Brinell hardness test using DigiRock Blue Hardness Tester with a ball diameter of 2.5 mm and ball load of 31.25 N. In order to examine hardness behaviour of control and composite samples, three indentations left marked on the surfaces of these samples. These marks were examined by optical microscope and average of these marks were calculated. For the perform hardness test of these samples, these averaged diameters were calculated following Equation (1),

$$HB = \frac{2P}{\pi D(D - \sqrt{D^2 - d^2})} \quad (1)$$

For this Equation (1), D is averaged diameter of marks (mm) and d is diameter of steel ball (mm). P is applied load in kg. HB is calculated Brinell hardness and unit of this hardness is  $\text{N/mm}^2$ .

Density and porosity measurements were applied via Archimedes water displacement test with SCALTEC sec31 balance device with an accuracy of 0.001 g using pure water at room temperature. Control and composite samples were firstly dry weighted ( $W_D$ ), Then, samples waited in the pure water for 24 h. After 24 h, these samples were dried with blotting paper and weighted in suspended air ( $W_A$ ), and in water ( $W_w$ ), respectively. Bulk density, apparent porosity and water absorption values were calculated by following Equations (2-4), using obtained experimental weighted results.

$$\text{Bulk density}(\text{g}/\text{mm}^3) = \frac{W_D}{W_A - W_w} \quad (2)$$

$$\text{Apparent Porosity} (\%) = \frac{100(W_A - W_D)}{W_A - W_w} \quad (3)$$

$$\text{Water absorption} (\%) = \frac{100(W_A - W_D)}{W_D} \quad (4)$$

Morphological and microstructural properties of this composite sample were examined using optic microscopy (OM) using Nikon Eclipse MA100, Scanning Electron Microscope (SEM) images, and Energy Dispersive Spectrometry (EDS) by FEI Quanta 650 Field Emission SEM device. The crystal structure of this sample was determined via PANalytical Empyrean X-ray 144 diffraction (XRD) with degree of  $10-90^\circ$  tube voltage of 45 kV, tube current of 40 mA and scanning rate of  $0.013^\circ/\text{min}$ , anode material of  $\text{Cu-K}\alpha$  ( $\lambda=1.54 \text{ \AA}$ )

## 3. Results and discussion

Figure 1 shows the OM images of control Alumix 431 sample (a) and Alumix 431 mixing with 15 wt% glass powder sample (b). It observed that the distribution of glass powder particles in this matrix alloy is homogeneous. The microstructure of this sample included of distributed fine and coarse glass powder particles. This can be related to good wettability of glass powder in the Alumix 431 matrix alloy [22]. With adding of glass powder, homogeneous distribution of the composite sample occurred because of good binding among particles of glass powder and matrix alloy [19]. OM image of this composite sample also shows the agglomeration due to accumulating effect and this homogeneous distribution of particles, good bonding and material hardening [19].

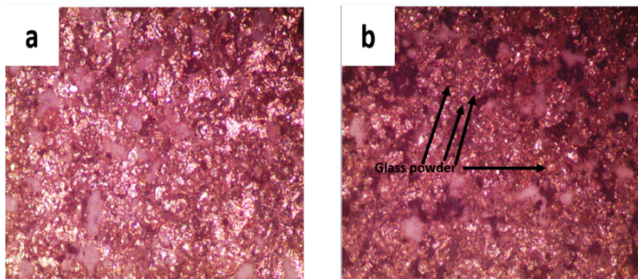


**Figure 1.** The OM images of control Alumix 431 sample (a) and Alumix 431-15% GP composite sample (b). (50x Magnification)

Figure 2 shows the SEM images of control Alumix 431 alloy (a and b) and Alumix 431 alloy blending with 15 wt% glass powder sample (c and d) ((a-c, 1 000x magnification) (b-d, 5 000x magnification)). Also, the EDS spectrums of control Alumix 431 alloy (a) and Alumix 431 alloy blending with 15 wt% glass powder (b) are given in Figure 3. The dark phase suited to Alumix 431 matrix alloy, while the bright particles corresponded to the glass powder particles which riched in Si, Ca, Na, Mg metallic elements [23]. It was observed that adding glass powder particles uniformly distributed into the Alumix 431 matrix alloy. Particle agglomeration and pores also observed. The main consideration for the agglomeration of the big particles is that big particles may be simply removed and bonded to neighbour particles because of shear stress [23]. The occurring of pores occurred from high regional stress concentration resulted from big particle and interfacial binding [23]. Matrix alloy includes mainly of  $\alpha$ -Al phase which consists of Zn, Mg and Cu elements as seen in Figure 3 (a) and (b). Phases on the grain boundaries are observed. These phases are at large amount of alloying elements (Al,  $Al_2CuMg$ ,  $MgZn_2$ ). Small sized phases on the grain boundaries are occurred from solid solution elements (Cu, Mg and Zn) in main primary phase [24]. This is observed on the SEM image and EDS spectrums of this samples that microstructure of composite sample shows dendritic structure of  $\alpha$ -Al. According to literature, this dendritic structure of  $\alpha$ -Al with secondary dendritic structures occur [25].

The microstructure of this composite material discloses a homogeneous distribution of the dispersoid into the matrix [25, 26]. This homogeneous distribution of dispersoid causes to improve mechanical and physical properties of this sample. This case is resulted from matrix plasticization that occurred from filling up of microvoids [25]. Sintering process of this composite sample includes of two stages [27]. First stage is occurred at temperature range from 50 to 500°C. The glass compacts shrink however shape of this compact does not vary. Glass powder with matrix alloy are pressed at room temperature and not sintered at higher temperatures. Pores on the surface of this composite samples occur. When sintering temperature increases, the surface of glass powder and matrix alloy particles are reacted and glass particles shrink to decrease the surface energy. As sintering temperature continue to increase, at the softening point of glass powder (approximately 550-620°C), glass powder softens and begins to deform into viscous droplets. The mixture of occurred droplets and solids closes to pores and glass powder platens shrinks [27]. Second stage is occurred at temperature range of 550-650°C. As temperature increases, viscosity of glass powder particles decreases and melted glass flows [27]. Pressed and sintered composite sample has hemispherical shape. The molten glass begins to diffuse under wetting tension and surface of this composite sample has platen structures [27]. On the

Figure 2(c) and Figure 3(b), it is observed that Mg element presence on the grain boundaries and surface of glass powder. This existence causes to good bonding. Throughout solidification, pushing of the solid Alumix 431 matrix alloy – molten glass powder interface and migrating alloying elements into the grain boundaries, and also separating dispersoid particles are seen. This improves the physical properties of this sample [26]. Density difference between matrix and adding material has a role on the distribution of adding material due to enough blending [28]. Less accumulating glass powder particles decrease viscosity. SEM and OM images of composite sample revealed formation of pores and clusters of glass powder due to higher viscosity [28]. On the surface of composite sample, needle shaped structures are also showed due to include of more calcium and alkali content in chemical composition of glass powder [29].

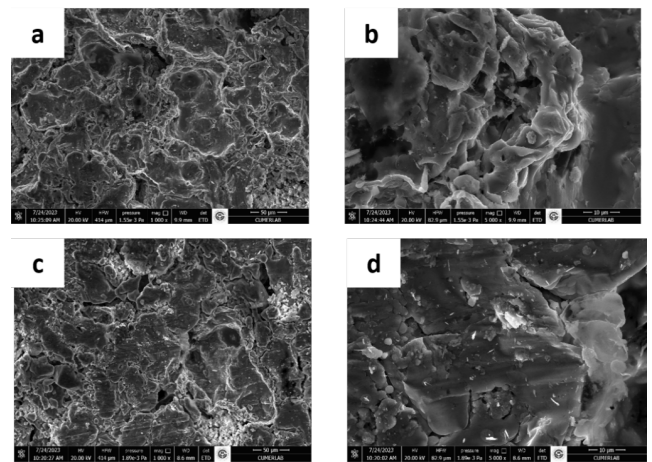


**Figure 2.** The SEM images of control sample (a,b) and Alumix 431-15%GP (c,d) composite sample. (a and c with 1 000x magnification, b and d with 5 000x magnification)

Table 1 gives The Brinell Hardness ( $N/mm^2$ ), Bulk density ( $g/cm^3$ ), Apparent porosity (%) and Water Absorption (%) values of control Alumix 431 sample and Alumix 431 -15%GP composite material. Glass powder added to Alumix 431 alloy, Brinell hardness and bulk density of this alloy increased as 41.846  $N/mm^2$ , 2.451  $g/cm^3$ , respectively, while apparent porosity and water absorption values of this sample decreased as 2.293% and 0.935%, respectively. In addition, decreased porosity clearly appears from SEM images of these samples in Figure 2. Addition of glass powder in the Alumix 431, hardness and density values of this composite sample improved due to glass powder functioned as additional materials block movements of dislocations into the Alumix 431 matrix. The dislocation mobility increases around particles in order to induce higher strength performance of this composite sample, with various mechanisms, dislocation folds and bumps or Orowan mechanism [30]. Including of high amount of ceramic silica and brittle alumina contents in the chemical composition of glass powder has a role on the blocking of flowability of the material [30, 31]. Additional glass powder into the Alumix 431 alloy leads to decreases softness of matrix alloy, while increasing hardness of this alloy. Related to brittle glass powder particulates, the surface of this soft matrix alloy is in contact with an abrasive particle surface [30]. Decreasing of porosity of this composite sample can occurred from formation of glass powder in the matrix with larger particle size, due to agglomerated glass powder [30]. Increasing hardness of



composite sample according to hardness value of control sample can showed that a good interfacial bonding between glass powder and matrix alloy. Comparing to literature, it is observed that hardness of this composite sample has small value. Due to applying low pressure (0.6-ton shock pressure), i) weak binding interaction with glass powder and matrix powder particles occurred [19]. ii) the density variety on glass powder (2.26-2.55 g/cm<sup>3</sup>) and matrix alloy (2.786 g/cm<sup>3</sup>, Alumix 431) causes to increase hardness value of this composite sample when adding glass powder into the matrix alloy [19]. This is show no good chemical reaction between matrix and adding material, agglomeration of grain occurred for the this composite material [19]. iii) lower hardness properties of matrix alloy and adding material, iv) the low weight percentage of glass powder is applied as adding material [19]. It is considered that if the more glass powder is utilized in the matrix alloy, the hardness value of obtained composite sample will be increased and also improve tribological properties of this composite samples. With adding of glass powder, the destruction of gaps leads to improve the hardness and density properties and decrease porosity and water absorption values of this sample [19]. Improving physical properties of this composite sample increases grain boundary areas because of grain refinement [32], and also resistance to indentation of indenter tips on the surface of sintered composite sample and showing plastic deformation of composite sample [33]. According to Hall-Petch relation, refining granular size can improve grain boundary area and remove of dislocation [33] and thus increase hardness value of this sample. Examining EDS spectrums of both of samples, Mg contents of these samples are roughly the same amount, but Cu content of control sample and composite sample are 3.08 wt% and 4.77 wt%, respectively. Increasing of hardness of this composite sample can also be related to high Cu content [33]. It assumed that the hardness will be increase to even higher values and better structural properties

will be obtained according to literature, if higher pressures are applied.

Figure 4 gives the XRD diffraction patterns of control Alumix 431 sample and Alumix 431 -15%GP composite material. For control Alumix 431 sample,  $\alpha$ -Al as primary main phase, MgZn<sub>2</sub> and Al<sub>2</sub>CuMg as secondary and tertiary main phases were recorded.  $\alpha$ -Al phase peaks for  $2\theta$  angles of 38.41°, 44.72°, 65.07°, 78.24°, 82.56° were determined, MgZn<sub>2</sub> phase peaks for  $2\theta$  angles of 34.41°, 35.49°, 42.82°, 47.62°, 62.28°, 68.25°, 78.52° and Al<sub>2</sub>CuMg phase peaks for  $2\theta$  angles of 31.71°, 36.13°, 56.46° were recorded [8, 34-42]. For composite sample,  $\alpha$ -Al as primary main phase, MgZn<sub>2</sub> as secondary main phases, Al<sub>2</sub>CuMg, diopside and cristobalite as other phases were recorded.  $\alpha$ -Al phase peaks for  $2\theta$  angles of 38.33°, 44.64°, 65.02°, 78.16°, 82.34° were determined, MgZn<sub>2</sub> phase peaks for  $2\theta$  angles of 34.35°, 42.75°, 47.15°, 62.18°, 67.88°, 78.43° and Al<sub>2</sub>CuMg phase peaks for  $2\theta$  angles of 31.65°, 56.00° were recorded [8, 34-42]. Adding of glass powder, peaks of  $\alpha$ -Al, MgZn<sub>2</sub> and Al<sub>2</sub>MgCu phase shifted to left side according to control sample. Diopside phase (CaMgO<sub>6</sub>Si<sub>2</sub>) peaks for  $2\theta$  angles of 28.28° and 56.50° and cristobalite (SiO<sub>2</sub>) phase peaks for  $2\theta$  angles of 36.13° were determined [10, 43-45]. MgZn<sub>2</sub> and Al<sub>2</sub>CuMg phases possess hexagonal close packed and orthorhombic crystal structures. Both of these phases have eutectic structures [42]. These phases have role on the improving of mechanical and physical properties of the alloy due to blocking effect of dislocation movement [35, 37-41]. Cristobalite phase occurs due to reaction enthalpy, which linked to the change of absorbed heat in the form of thermal energy to kinetic energy in order that forming ionic diffusion in the microstructures of materials. This phase forms, when sintering temperature increases [10]. Small sized diopside phases embedded in glassy structure [45].

**Table 1.** The Brinell Hardness, Bulk density, Apparent porosity and Water Absorption values of control Alumix 431 sample and Alumix 431 -15%GP composite material.

|                  | Brinell Hardness<br>N/mm <sup>2</sup> | Bulk density (g/cm <sup>3</sup> ) | Apparent porosity (%) | Water absorption<br>(%) |
|------------------|---------------------------------------|-----------------------------------|-----------------------|-------------------------|
| Alumix 431       | 29.679                                | 2.372                             | 8.710                 | 3.669                   |
| Alumix 431-15%GP | 41.846                                | 2.451                             | 2.293                 | 0.935                   |

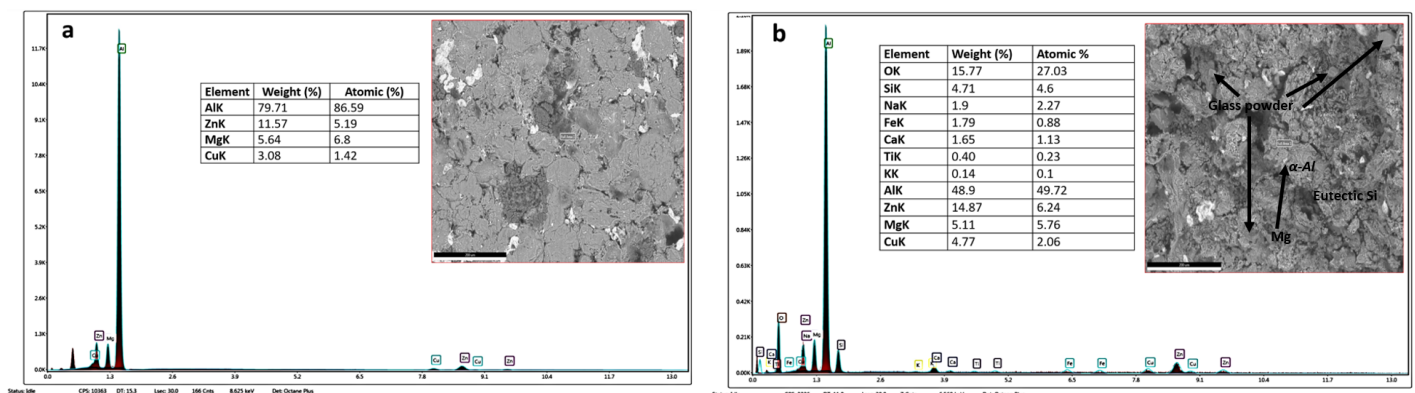


**Figure 3.** The EDS spectrums of control Alumix 431 sample (a) and Alumix 431-15%GP composite sample (b)

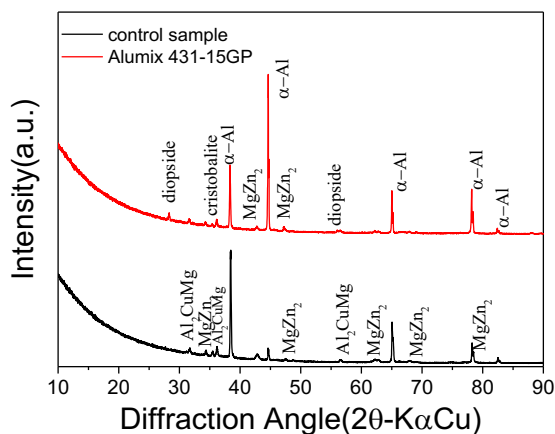


**Figure 4.** The XRD patterns of control Alumix 431 and Alumix 431-15%GP composite samples

### Conclusion

In this study, physical and microstructural properties of Alumix 431 alloy mixing with 15% glass powder produced via powder metallurgy method. Following results are given:

- i. Adding of glass powder into the matrix alloy, hardness and bulk density of composite sample are improved while porosity and water absorption of this sample decreased.
- ii. Glass powder in the structure of matrix alloy has homogeneous distribution and agglomeration due to good bonding between glass powder particles and matrix alloy.
- iii. Diopside and cristobalite phases with  $MgZn_2$ ,  $Al_2CuMg$  occurred.

### Acknowledgement

Authors are greatly thankful to Cukurova University Research Funding (FBA-2021-13966).

### Authorship contributions

Ayşe Nur Acar: conceptualization, methodology, validation, formal analysis, investigation, resources, writing - original draft, writing - review & editing, visualization.

Dogan Kaya: conceptualization, methodology, validation, formal analysis, investigation, resources, writing - original draft, writing - review & editing, visualization.

Abdul Kadir Ekşi: conceptualization, methodology, validation, resources, writing - original draft, writing - review & editing, visualization, supervision.

Ahmet Ekicibil: conceptualization, methodology, validation, resources, writing - original draft, writing - review & editing, visualization, supervision.

### References

1. Azadbeh, M., Razzaghi, Z.A., Properties evolution during transient liquid phase sintering of PM Alumix 431, *Advances in Materials Science and Engineering*, **2009**, 648906
2. Lee, E., Oak, J.J., Kim, Y., Park, Y., Effect of Added Gas-Atomized Al-Si/SiC p Composite Powder on the Sinterability and Mechanical Properties of Alumix 431 fabricated by Hot-Pressing Process, *Korean Journal of Metals and Materials*, **2017**, 55(2):98-109
3. Zhou, B., Liu, B., Zhang, S., The advancement of 7xxx series aluminum alloys for aircraft structures: A review, *Metals*, **2021**, 11(5):718

4. Yu, B.C., Bae, K.C., Jung, J.K., Kim, Y.H., Park, Y.H., Effect of heat treatment on the microstructure and wear properties of Al-Zn-Mg-Cu/in-situ Al-9Si-SiCp/pure Al composite by powder metallurgy, *Metals and Materials International*, **2018**, 24, 576-585
5. Eksi, A., Veltl, G., Petzoldt, F., Lipp, K., Sonsino, C., Tensile and fatigue properties of cold and warm compacted Alumix 431 alloy, *Powder metallurgy*, 2004, 47(1): 60-64
6. Schaffer, G., Huo, S., On development of sintered 7xxx series aluminum alloys, *Powder Metallurgy*, **1999**, 42(3):219-226
7. Acar, A.N., Mutlu, R.N., Kaya, D., Ekşi, A.K., Ekicibil, A., Fe addition influence on the mechanical and thermophysical behaviours of PM Alumix 431 alloy, *Journal of Molecular Structure*, **2021**, 130031
8. Rudianto, H., Jang, G., Yang, S., Kim, Y., Dlouhy, I., Effect of SiC particles on sinterability of Al-Zn-Mg-Cu P/M alloy, *Archives of Metallurgy and Materials*, **2015**, 60(2):1382-1385
9. Leszczyńska-Madej, B., Madej, M., Wąsik, A., Analysis of sintering process of Alumix431-B4C composites, *Journal of Alloys and Compounds*, **2023**, 171362
10. Souza, A.C., Pereira, M.F., Mossin, L.C., Thermal and mechanical characterization of blindex glass powder residue® for the production of ecological coating, *Journal of Materials Research and Technology*, **2021**, 1794-1803
11. Zhang, H., Hu, Y., Hou, G., An, Y., Liu, G., The effect of high-velocity oxy-fuel spraying parameters on microstructure, corrosion and wear resistance of Fe-based metallic glass coatings, *Journal of non-crystalline solids* **2014**, 406, 37-44
12. Hasanuzzaman, M., Rafferty, A., Sajjia, M., Olabi, A.-G., Properties of glass materials, *Reference Module in Materials Science and Materials Engineering*, **2016**, 647-657
13. Saify, S., Radhi, M.S., Al-Mashhadi, S.A., Mareai, B., Jabr, S.F., Mohammed, Z.A., Al-Khafaji, Z., Al-Husseinawi, F., Impact of waste materials (glass powder and silica fume) on features of high-strength concrete, *Open Engineering*, **2023**, 13(1):20220479
14. Setina, J., Gabrene, A., Juhnevcia, I., Effect of pozzolanic additives on structure and chemical durability of concrete, *Procedia Engineering*, **2013**, 57, 1005-1012
15. Martin, J.W., Glasses and ceramics, in: J.W. Martin (Ed.), *Materials for Engineering (Third Edition)*, Woodhead Publishing, **2006**, 133-158
16. Lee, J.E., Kim, E., Hwang, J.B., Choi, J.C., Lee, J.K., Flake formation and composition in soda-lime-silica and borosilicate glasses, *Heliyon*, **2023**, 9(6)
17. Gruben, G., Vysochinskiy, D., Coudert, T., Reyes, A., Lademo, O.G., Determination of Ductile Fracture Parameters of a Dual-Phase Steel by Optical Measurements, *Strain*, **2013**, 49(3):221-232
18. Sander, G., Jiang, D., Wu, Y., Birbilis, N., Exploring the possibility of a stainless steel and glass composite produced by additive manufacturing, *Materials & Design*, **2020**, 196, 109179
19. Wubieneh, T.A., Tegegne, S.T., Fabrication and Characterization of Aluminum (Al-6061) Matrix Composite Reinforced with Waste Glass for Engineering Applications, *Journal of Nanomaterials*, **2022**, 8409750

20. Hoseini, M., Meratian, M., Fabrication of in situ aluminum–alumina composite with glass powder, *Journal of Alloys and Compounds*, **2009**, 471(1): 378-382
21. Kumar, D.R., Loganathan, C., Narayanasamy, R., Effect of glass in aluminum matrix on workability and strain hardening behavior of powder metallurgy composite, *Materials & Design*, **2011**, 32(4): 2413-2422
22. Bharanidaran, R., Evaluation of hardness and impact strength of aluminium alloy (LM6)–soda–lime composite, *Australian Journal of Mechanical Engineering*, **2021**, 19(2):196-201
23. Xie, M., Wang, Z., Zhang, G., Yang, C., Zhang, W., Prashanth, K., Microstructure and mechanical property of bimodal-size metallic glass particle-reinforced Al alloy matrix composites, *Journal of Alloys and Compounds*, **2020**, 814, 152317
24. Chen, G., Chen, Q., Wang, B., Du, Z., Microstructure evolution and tensile mechanical properties of thixoformed high performance Al-Zn-Mg-Cu alloy, *Metals and Materials International*, **2015**, 21, 897-906
25. Hiremath, A., Hemanth, J., Experimental evaluation of the coefficient of thermal expansion of chilled aluminum alloy-borosilicate glass (P) composite, *J Mater Environ*, **2017**, 8(12), 4246-4252
26. Hemanth, J., Wear behavior of chilled (metallic and non-metallic) aluminum alloy–glass particulate composite, *Materials & design*, **2002**, 23(5), 479-487
27. Hou, L., Liu, S., Zhu, X., Interaction of Glass Powder with Al Powder and Zinc Oxide in Aluminum Paste, *Coatings*, **2024**, 14(1):64
28. Bhowmik, A., Meher, A., Biswas, S., Dey, D., Kumar, M.S., Biswas, A., Alsharabi, R.M., Synthesis and Characterization of Borosilicate Glass Powder-Reinforced Novel Lightweight Aluminum Matrix Composites, *Advances in Materials Science and Engineering*, **2022**, 9487900
29. Qin, D., Hu, Y., Li, X., Waste glass utilization in cement-based materials for sustainable construction: A review, *Crystals*, **2021**, 11(6):710
30. Adediran, A.A., Akinwande, A.A., Balogun, O.A., Adesina, O.S., Olayanju, A., Mojisola, T., Evaluation of the properties of Al-6061 alloy reinforced with particulate waste glass, *Scientific African*, **2021**, 12
31. Sharma, P., Sharma, S., Khanduja, D., Production and some properties of Si<sub>3</sub>N<sub>4</sub> reinforced aluminium alloy composites, *Journal of Asian Ceramic Societies*, **2015**, 3(3):352-359
32. Yc, M.K., Shankar, U., Evaluation of mechanical properties of aluminum alloy 6061-glass particulates reinforced metal matrix composites, *International Journal of Modern Engineering Research*, **2012**, 2(5):3207-3209
33. Shu, W., Hou, L., Zhang, C., Zhang, F., Liu, J., Liu, J., Zhuang, L., Zhang, J., Tailored Mg and Cu contents affecting the microstructures and mechanical properties of high-strength Al–Zn–Mg–Cu alloys, *Materials Science and Engineering: A*, **2016**, 657, 269-283
34. Li, X., Yu, J., Modeling the effects of Cu variations on the precipitated phases and properties of Al-Zn-Mg-Cu alloys, *Journal of Materials engineering and Performance*, **2013**, 22, 2970-2981
35. Rudianto, H., Jang, G.J., Yang, S.S., Kim, Y.J., Dlouhy, I., Evaluation of sintering behavior of premix Al-Zn-Mg-Cu alloy powder, *Advances in Materials Science and Engineering*, **2015**, 987687
36. Mondal, C., Mukhopadhyay, A., On the nature of T (Al<sub>2</sub>Mg<sub>3</sub>Zn<sub>3</sub>) and S (Al<sub>2</sub>CuMg) phases present in as-cast and annealed 7055 aluminum alloy, *Materials Science and Engineering: A*, **2005**, 391(1-2):367-376
37. Lin, Y., Jiang, Y.-Q., Xia, Y.-C., Zhang, X.-C., Zhou, H.-M., Deng, J., Effects of creep-aging processing on the corrosion resistance and mechanical properties of an Al–Cu–Mg alloy, *Materials Science and Engineering: A*, **2014**, 605, 192-202
38. Wang, J.-q., Zhang, B., Wu, B., Ma, X., Size-dependent role of S phase in pitting initiation of 2024Al alloy, *Corrosion Science*, **2016**, 105, 183-189
39. Hashimoto, T., Zhang, X., Zhou, X., Skeldon, P., Haigh, S., Thompson, G., Investigation of dealloying of S phase (Al<sub>2</sub>CuMg) in AA 2024-T3 aluminium alloy using high resolution 2D and 3D electron imaging, *Corrosion science*, **2016**, 103, 157-164
40. Lacroix, L., Blanc, C., Pébère, N., Thompson, G., Tribollet, B., Vivier, V., Simulating the galvanic coupling between S-Al<sub>2</sub>CuMg phase particles and the matrix of 2024 aerospace aluminium alloy, *Corrosion Science*, **2012**, 64, 213-221
41. Shi, H., Tian, Z., Hu, T., Liu, F., Han, E.-H., Taryba, M., Lamaka, S., Simulating corrosion of Al<sub>2</sub>CuMg phase by measuring ionic currents, chloride concentration and pH, *Corrosion Science*, **2014**, 88, 178-186
42. Schaffer, G.B., Yao, J.-Y., Bonner, S., Crossin, E., Pas, S.J., Hill, A.J., The effect of tin and nitrogen on liquid phase sintering of Al–Cu–Mg–Si alloys, *Acta Materialia*, **2008**, 56(11):2615-2624
43. Acar, A.N., Kaya, D., Ekşi, A.K., Ekicibil, A., Structural and Surface Properties of Glass Powder Coated Cr Steels, *The International Journal of Materials and Engineering Technology*, **2021**, 4(2):109-116
44. Samad, H.A., Jaafar, M., Othman, R., Kawashita, M., Razak, N.H.A., New bioactive glass-ceramic: synthesis and application in PMMA bone cement composites, *Bio-medical materials and engineering*, **2011**, 21(4):247-258
45. Rawlings, R., Wu, J., Boccaccini, A., Glass-ceramics: their production from wastes—a review, *Journal of materials science*, **2006**, 41, 733-761